Assembly of a Robust, Thermally Stable Porous Cobalt(II) Nicotinate Framework Based on a Dicobalt Carboxylate Unit

Yen-Hsiang Liu,[†] Hui-Lien Tsai,[‡] Yi-Long Lu,[†] Yuh-Sheng Wen,[†] Ju-Chun Wang,[§] and Kuang-Lieh Lu*[,†]

Institute of Chemistry, Academia Sinica, Taipei 115, Taiwan, ROC, Department of Chemistry, National Cheng Kung University, Tainan 701, Taiwan, ROC, and Department of Chemistry, Soochow University, Taipei 100, Taiwan, ROC

Received May 28, 2001

A series of robust, thermally stable open-framework cobalt nicotinate compounds, $Co_2(H_2O)(C_6H_4O_2N)_4 \cdot 0.5CH_3CH_2OH \cdot 0.5H_2O$ (**1**), $Co_2(H_2O)(C_6H_4O_2N)_4$ (**2**), and $Co_2(H_2O)(C_6H_4O_2N)_4 \cdot C_6H_5CH_2OH$ (**3**), based on rigid dimetallic carboxylate clusters as the basic building unit have been prepared. Single-crystal X-ray crystallographic analyses of **1** and **3** reveal the host framework possessing an effective channel area with the dimensions of 10.8 × 4.5 Å. These channels can accommodate guest molecules of various sizes and shapes such as ethanol, water, and benzyl alcohol. Thermogravimetric analysis shows a two-step weight loss corresponding to the loss of guest molecules followed by the loss of coordinated water. The host framework is thermally stable up to 295 °C. The cobalt nicotinate host remains intact, even upon the removal of the guest to form compound **2** as revealed by single-crystal X-ray diffraction analysis. Crystal data for **1**: $Co_2(H_2O)(C_6H_4O_2N)_4 \cdot 0.5CH_3CH_2OH \cdot 0.5H_2O$, fw = 656.33, triclinic, space group $P\bar{1}$, $a = 10.5407(2)$ Å, $b = 11.8266(3)$ Å, $c = 14.1122(2)$ Å, $\alpha = 106.878(4)°$, $\beta = 102.411(2)°$, $\gamma = 111.011(3)°$, $V = 1467.9(5)$ Å^3, $Z = 2$. Crystal data for **2**: $Co_2(H_2O)(C_6H_4O_2N)_4$, fw = 624.28, triclinic, space group $P\bar{1}$, $a = 10.507(3)$ Å, $b = 11.824(2)$ Å, $c = 14.113(3)$ Å, $\alpha = 107.06(2)°$, $\beta = 102.39(2)°$, $\gamma = 111.105(16)°$, $V = 1459.5(6)$ Å^3, $Z = 2$. Crystal data for **3**: $Co_2(H_2O)(C_6H_4O_2N)_4 \cdot C_6H_5CH_2OH$, fw = 732.42, triclinic, space group $P\bar{1}$, $a = 10.6671(6)$ Å, $b = 12.0063(7)$ Å, $c = 14.0658(8)$ Å, $\alpha = 106.7180(10)°$, $\beta = 102.2790(10)°$, $\gamma = 111.1900(10)°$, $V = 1504.1(6)$ Å^3, $Z = 2$. The magnetic exchange coupling between the dicobalt centers for compounds **1** and **3** are analyzed on the basis of both the Curie−Weiss expression and a binuclear magnetic model. The negative values of the magnetic exchange coupling constant indicate the antiferromagnetic nature within the cobalt dimer.

Introduction

One of the major challenges in the design and synthesis of porous metal−organic framework ("zeolite-analogue") materials is to maintain the host framework integrity in the absence of guests in order to allow for reversible access to the cavities within the host. Extensive studies have been carried out on the synthesis and tailor design of these functional coordination polymers, adopting the concept of supramolecular self-assembly[1−20]because of their diverse structural properties and potential applications in the field of size-selective separation, gas adsorption, and catalysis.[21−27]

One of the approaches to meet the above challenge is to employ more rigid building-block entities in the framework to enhance the robustness. Recent studies demonstrated that the construction of metal carboxylate clusters provided an effective strategy to form robust hosts possessing porosity.[28−32] A few successful examples are the $Zn_4(O)O_{12}C_6$ cluster unit observed

* To whom correspondence should be addressed. Phone: +886-2-27898518. Fax: +886-2-27831237. E-mail: lu@chem.sinica.edu.tw.
† Academia Sinica.
‡ National Cheng Kung University.
§ Soochow University.

(1) Lehn, J. M.; Atwood, J. L.; Davies, J. E. D.; MacNicol, D. D.; Vögtle, F. *Comprehensive Supramolecular Chemistry*; Toda, F., Bishop, R., Eds.; Pergamon: Oxford, 1996; Vol. VI.
(2) Robson, R. *J. Chem. Soc., Dalton Trans.* **2000**, 3735.
(3) Kitagawa, S.; Kondo, M. *Bull. Chem. Soc. Jpn.* **1998**, *71*, 1735.
(4) Zaworotko, M. J. *Angew. Chem., Int. Ed.* **2000**, *39*, 3052.
(5) Eddaoudi, M.; Moler, D. B.; Li, H.; Chen, B.; Reineke, T. M.; O'Keeffe, M.; Yaghi, O. M. *Acc. Chem. Res.* **2001**, *34*, 319.
(6) Pecoraro, V. L.; Bodwin, J. J.; Cutland, A. D. *J. Solid State Chem.* **2000**, *152*, 68.
(7) Chui, S. S.-Y.; Lo, S. M.-F.; Charmant, P. H.; Orpen, A. G.; Williams, I. D. *Science* **1999**, *283*, 1148.
(8) Lee, H.; Laine, A.; O'Keeffe, M.; Yaghi, O. M. *Science* **1999**, *111*, 190.
(9) Kondo, M.; Okubu, T.; Asami, A.; Noro, S.; Yoshitomi, T.; Kitagawa, S.; Ishii, T.; Matsuzaka, H.; Seki, K. *Angew. Chem., Int. Ed.* **1999**, *38*, 140.
(10) Min, K. S.; Suh, M. P. *Chem. Eur. J.* **2001**, *7*, 303.
(11) Zaworotko, M. *Nature* **1999**, *402*, 242.
(12) Dong, Y.-B.; Smith, M. D.; zur Loye, H.-C. *Angew. Chem., Int. Ed.* **2000**, *39*, 4271.
(13) Keller, S. W. *Angew. Chem., Int. Ed. Engl.* **1997**, *36*, 247.
(14) Evans, O. R.; Lin, W. *Inorg. Chem.* **2000**, *39*, 2189.
(15) Pan, L.; Huang, X.; Li, J.; Wu, Y.; Zheng, N. *Angew. Chem., Int. Ed.* **2000**, *39*, 527.
(16) Lee, E.; Kim, J.; Heo, J.; Whang, D.; Kim, K. *Angew. Chem., Int. Ed.* **2001**, *40*, 399.
(17) Reineke, T. M.; Eddaoudi, M.; Moler, D.; O'Keeffe, M.; Yaghi, O. M. *J. Am. Chem. Soc.* **2000**, *122*, 4843.
(18) Robson, R.; Batten, S. R. *Angew. Chem., Int. Ed.* **1998**, *37*, 1460.
(19) Liu, Y.-H.; Lin, C.-S.; Chen, S.-Y.; Tsai, H.-L.; Ueng, C.-H.; Lu, K.-L. *J. Solid State Chem.* **2001**, *157*, 166.
(20) Liu, Y.-H.; Lu, Y.-L.; Tsai, H.-L.; Wang, J.-C.; Lu, K.-L. *J. Solid State Chem.* **2001**, *158*, 315.
(21) Kiang, Y.-H.; Garner, G. B.; Lee, S.; Xu, Z.; Lobkovsky, E. B. *J. Am. Chem. Soc.* **1999**, *121*, 8204.
(22) Tabares, L. C.; Navarro, J. A. R.; Salas, J. M. *J. Am. Chem. Soc.* **2001**, *123*, 383.
(23) Noro, S.; Kitagawa, S.; Kondo, M.; Seki, K. *Angew. Chem., Int. Ed.* **2000**, *39*, 2081.

10.1021/ic010528k CCC: $20.00
Published on Web 10/31/2001

in zinc(II) benzenedicarboxylates,[28] the $Cu_2(O_2C)_4$ cluster unit observed in copper(II) 1,3,5,7-adamantanetetracarboxylates,[31] and the $Zn_3(O)(O_2C)_6$ cluster in the case of a zinc(II) coordination polymer possessing chiral channels.[32] However, the strategic design of tailored coordination polymers with "predictable" structure-based properties is still in its early stage. Much remains to be done to attain this goal. Expanding on this approach, we report here a series of open-framework coordination polymers: $Co_2(H_2O)(C_6H_4O_2N)_4 \cdot 0.5CH_3CH_2OH \cdot 0.5H_2O$ (**1**), $Co_2(H_2O)(C_6H_4O_2N)_4$ (**2**), and $Co_2(H_2O)(C_6H_4O_2N)_4 \cdot C_6H_5CH_2OH$ (**3**). The host network of these compounds consists of a $Co_2(O)(O_2C)_2$ cluster unit that is linked by a rigid nicotinate ligand with good thermal stability. Their thermal stability, inclusion, and magnetic properties are also reported.

Experimental Section

Cobalt(II) nitrate hexahydrate and 3-cyanopyridine were purchased from ACROS Chemicals and used as received without further purification. Thermogravimetric (TG) analysis was performed under nitrogen on a Perkin-Elmer TGA-7 TG analyzer. Powder diffraction measurements were recorded on a Siemens D-5000 diffractometer at 40 kV, 30 mA for Cu Kα ($\lambda = 1.5406$ Å), with a step size of 0.02° in θ and a scan speed of 1 s per step size. Variable-temperature dc magnetic susceptibility data were collected for polycrystalline samples of complexes **1** and **3** in an applied field of 1.0 kG and in the temperature range of 2.0−300.0 K, which were measured by a SQUID magnetometer (Quantum Design, MPMS-7). The samples were embedded in eicosane wax to prevent any torquing of the polycrystalline in the magnetic field. Pascal's constants[33] were used to estimate the diamagnetic corrections.

$Co_2(H_2O)(C_6H_4O_2N)_4 \cdot 0.5CH_3CH_2OH \cdot 0.5H_2O$ (1). Single crystals of **1** were synthesized by heating a mixture of $Co(NO_3)_2 \cdot 6H_2O$ (0.1 mmol) and 3-cyanopyridine (0.1 mmol) in the mixture of the solvents ethanol (1.25 mL) and water (3.75 mL) at 140 °C for 96 h. The solid product was washed by distilled water and isolated by suction filtration. The final product contained a single phase of red-lathy crystals of **1** in a yield of 58% based on nicotinate. A powder X-ray diffraction pattern of the bulk sample compared well with the pattern simulated from the single-crystal data (vide infra). Anal. Calcd: C, 45.75; H, 3.38; N, 8.54. Found: C, 45.40; H, 3.72; N, 8.35.

$Co_2(H_2O)(C_6H_4O_2N)_4$ (2). A single crystal of **2** was obtained by mounting a single crystal of **1** on a glass fiber and keeping it sealed in a Schlink tube under vacuum (10^{-3} Torr) for 12 h. The resulting crystal was sealed to prevent contact with the moisture from the air during the single-crystal X-ray diffraction analysis.

$Co_2(H_2O)(C_6H_4O_2N)_4 \cdot C_6H_5CH_2OH$ (3). Single crystals of **3** were synthesized following a procedure similar to that used for **1**. A mixture of $Co(NO_3)_2 \cdot 6H_2O$ (0.1 mmol) and 3-cyanopyridine (0.1 mmol) was dissolved in a mixed solvent of benzyl alcohol (1.25 mL) and water (3.75 mL) and heated at 140 °C for 96 h. The solid product was washed by distilled water and obtained by suction filtration. The final product contained a single phase of red-lathy crystals of **3** in a yield of 62% based on nicotinate. A powder X-ray diffraction pattern of the bulk sample compared well with the pattern simulated from the single-crystal data (vide infra). Anal. Calcd: C, 50.83; H, 3.57; N, 7.64. Found: C, 49.72; H, 3.52; N, 7.59.

Table 1. Crystallographic Data for **1**−**3**[a]

	1	**2**	**3**
chemical formula	$Co_2C_{25}H_{22}N_4O_{10}$	$Co_2C_{24}H_{18}N_4O_9$	$Co_2C_{31}H_{26}N_4O_{10}$
a, Å	10.5407(2)	10.507(3)	10.6671(6)
b, Å	11.8266(3)	11.824 (2)	12.0063(7)
c, Å	14.1122(2)	14.113(3)	14.0658(8)
α, deg	106.878(4)	107.06(2)	106.7180(10)
β, deg	102.411(2)	102.39(2)	102.2790(10)
γ, deg	111.011(3)	111.105(16)	111.1900(10)
V, Å^3	1467.9(5)	1459.5(6)	1504.1(6)
Z	2	2	2
fw	656.33	624.28	732.42
space group	$P\bar{1}$	$P\bar{1}$	$P\bar{1}$
T, °C	25(2)	25(2)	25(2)
λ, Å	0.710 73	0.710 73	0.710 73
D_{calcd}, g/cm^3	1.485	1.421	1.617
μ, cm^{-1}	11.89	11.89	11.70
R1	0.0336	0.0435	0.0348
wR2	0.1145	0.1584	0.1013

[a] $R1 = \sum\{||F_o| - |F_c||\}/\{\sum|F_o|\}$ and $wR2 = \{\sum[w(F_o^2 - F_c^2)^2]\}/\{\sum[w(F_o^2)^2]\}^{1/2}$.

Crystallographic Determination. A single crystal of **1** with the dimensions of 0.40 × 0.36 × 0.12 mm was mounted on the tip of a glass fiber and placed onto the goniometer head for indexing and intensity data collection. The measurements were performed on an Enraf-Nonius CAD4 diffractometer equipped with graphite-monochromatized Mo Kα radiation ($\lambda = 0.710\,73$ Å). Intensity data were collected at 293(2) K with the $\omega-2\theta$ scan method within the limits $2° < \theta < 26°$ and were monitored by three standards every 4 h. Lorentz polarization corrections were performed.[34] Empirical absorption corrections were based on ψ-scan data. On the basis of systematic absences and statistics of intensity distribution, the space group $P\bar{1}$ was determined. Direct methods were used to locate the cobalt atoms, with the remaining non-hydrogen atoms being found from successive difference Fourier maps. The structure was refined by full-matrix least-squares based on F^2 values. All of the non-hydrogen atoms on the cobalt nicotinate framework were subjected to anisotropic refinement. Hydrogen atoms on the bridging water were located from difference Fourier maps. All of the hydrogen atoms of the nicotinate groups were assigned by geometric placing. Because of the disorder nature of guest (water and ethanol) molecules, their oxygen and carbon atoms were located in electron density maps and were refined isotropically with a site-occupation factor (SOF) of 0.5 assigned for all of the oxygen and carbon atoms of the guest molecules. Their locations are only approximate. No attempt was made to locate the hydrogen atoms of the guest molecules. Computations were performed using the WINGX[35] and SHELX-97 program packages.[36]

To analyze compound **2**, the same crystal that was used for the crystallographic determination of **1** was first treated under a vacuum and then sealed. A crystallographic determination procedure similiar to that which was previously mentioned was performed. The results showed that only a negligible amount of the residual electron density of 0.96 e A^{-3} was observed from the difference Fourier map, indicating that guest molecules were removed in a vacuum.

A single crystal of **3** with the dimensions of 0.64 × 0.40 × 0.16 mm was selected for crystallographic analysis. Single-crystal data were collected on a Bruker SMART CCD diffractometer (Mo Kα, $\lambda = 0.710\,73$ Å) at $T = 298(2)$ K. The data were corrected for Lorentzian, polarization, and absorption effects. SHELX-97 was used for solving the structure and full-matrix least-squares refinement on F^2. The hydrogen atoms of the bridging water molecule were located from a difference map. The hydrogen atoms on nicotinate and the phenyl group of benzyl alcohol were assigned by a geometrical calculation. An SOF value of 0.5 was assigned to the disordered $-CH_2OH$ group of the benzyl alcohol molecule. Crystallographic details for all three of the compounds are listed in Table 1 and selected bond distances and angles in Table 2.

(24) Choi, H. J.; Lee, T. S.; Suh, M. P. *Angew. Chem., Int. Ed.* **1999**, *38*, 1405.
(25) Holman, K. R.; Pivovar, A. M.; Swift, J. A.; Ward, M. D. *Acc. Chem. Res.* **2001**, *34*, 107.
(26) Eddaoudi, M.; Li, H.; Yaghi, O. M. *J. Am. Chem. Soc.* **2000**, *122*, 1391.
(27) Kasai, K.; Aoyagi, M.; Fujita, M. *J. Am. Chem. Soc.* **2000**, *122*, 2140.
(28) Li, H.; Eddaoudi, M.; O'Keeffe, M.; Yaghi, O. M. *Nature* **1999**, *402*, 276.
(29) Chen, B.; Eddaoudi, M.; Hyde, S. T.; O'Keeffe, M.; Yaghi, O. M. *Science* **2001**, 291, 1021.
(30) Mori, W.; Takamizawa, S. *J. Solid State Chem.* **2000**, *152*, 120.
(31) Chen, B.; Eddaoudi, M.; Reineke, T. M.; Kampf, J. W.; O'Keeffe, M.; Yaghi, O. M. *J. Am. Chem. Soc.* **2000**, *122*, 11559.
(32) Seo, S. J.; Whang, D.; Lee, H.; Jun, S. I.; Oh, J.; Jeon, Y. J.; Kim. K. *Nature* **2000**, *404*, 982.
(33) Boudreaux, E. A.; Mulay, L. N. *Theory and Application of Molecular Paramagnetism*; John Wiley & Sons: New York, 1976.

Table 2. Selected Bond Lengths (Å) and Angles (deg) for **1**−**3**[a]

bond length (Å)		angle (deg)		angle (deg)	
		Compound **1**			
Co(1)−O(21)	2.046(2)	O(21)−Co(1)−O(41)	94.38(9)	O(31)#3−Co(2)−O(22)	86.87(9)
Co(1)−O(41)	2.100(2)	O(41)−Co(1)−O(11)#1	85.72(9)	O(42)−Co(2)−O(22)	97.25(9)
Co(1)−O(11)#1	2.113(2)	O(21)−Co(1)−N(31)	88.66(9)	O(31)#3−Co(2)−O(91)	90.84(9)
Co(1)−O(91)	2.166(2)	O(11)#1−Co(1)−N(31)	91.22(10)	O(42)−Co(2)−O(91)	88.73(8)
Co(1)−N(31)	2.137(3)	O(21)−Co(1)−N(41)#2	91.01(9)	O(22)−Co(2)−O(91)	90.23(8)
Co(1)−N(41)#2	2.145(2)	O(41)−Co(1)−N(41)#2	87.35(9)	O(31)#3−Co(2)−N(21)#4	88.62(9)
Co(2)−O(31)#3	2.077(2)	O(11)#1−Co(1)−N(41)#2	87.62(9)	O(42)−Co(2)−N(21)#4	92.00(9)
Co(2)−O(42)	2.081(2)	N(31)−Co(1)−N(41)#2	91.99(10)	O(22)−Co(2)−N(21)#4	86.92(9)
Co(2)−O(22)	2.112(2)	O(21)−Co(1)−O(91)	91.67(9)	O(31)#3−Co(2)−N(11)	88.83(9)
Co(2)−O(91)	2.152(2)	O(41)−Co(1)−O(91)	88.52(8)	O(42)−Co(2)−N(11)	87.07(9)
Co(2)−N(11)	2.201(2)	O(11)#1−Co(1)−O(91)	89.71(8)	O(91)−Co(2)−N(11)	92.20(9)
Co(2)−N(21)#4	2.153(3)	N(31)−Co(1)−O(91)	92.01(9)	N(21)#4−Co(2)−N(11)	90.61(10)
		Compound **2**			
Co(1)−O(21)	2.044(3)	O(21)−Co(1)−O(41)	94.30(12)	O(31)#3−Co(2)−O(22)	86.58(13)
Co(1)−O(41)	2.098(3)	O(41)−Co(1)−O(11)#1	85.75(12)	O(42)−Co(2)−O(22)	97.21(12)
Co(1)−O(11)#1	2.108(3)	O(21)−Co(1)−N(31)	88.68(13)	O(31)#3−Co(2)−N(21)#4	88.61(13)
Co(1)−O(91)	2.160(3)	O(11)#1−Co(1)−N(31)	91.25(13)	O(42)−Co(2)−N(21)#4	91.61(13)
Co(1)−N(31)	2.138(4)	O(21)−Co(1)−N(41)#2	90.96(13)	O(22)−Co(2)−N(21)#4	87.19(12)
Co(1)−N(41)#2	2.140(3)	O(41)−Co(1)−N(41)#2	87.46(12)	O(31)#3−Co(2)−O(91)	91.09(12)
Co(2)−O(31)#3	2.073(3)	O(11)#1−Co(1)−N(41)#2	87.53(12)	O(42)−Co(2)−O(91)	88.86(12)
Co(2)−O(42)	2.075(3)	N(31)−Co(1)−N(41)#2	91.89(14)	O(22)−Co(2)−O(91)	90.12(12)
Co(2)−O(22)	2.102(3)	O(21)−Co(1)−O(91)	91.71(12)	O(31)#3−Co(2)−N(11)	89.27(13)
Co(2)−O(91)	2.153(3)	O(41)−Co(1)−O(91)	88.69(11)	O(42)−Co(2)−N(11)	86.94(12)
Co(2)−N(11)	2.195(3)	O(11)#1−Co(1)−O(91)	89.81(12)	N(21)#4−Co(2)−N(11)	90.77(13)
Co(2)−N(21)#4	2.151(4)	N(31)−Co(1)−O(91)	91.83(13)	O(91)−Co(2)−N(11)	91.91(12)
		Compound **3**			
Co(1)−O(21)	2.0525(17)	O(21)−Co(1)−O(41)	92.90(7)	O(31)#3−Co(2)−O(22)	88.30(7)
Co(1)−O(41)	2.1007(17)	O(41)−Co(1)−O(11)#1	86.13(7)	O(42)−Co(2)−O(22)	98.65(7)
Co(1)−O(11)#1	2.1268(17)	O(21)−Co(1)−N(31)	88.62(7)	O(31)#3−Co(2)−O(91)	89.23(7)
Co(1)−O(91)	2.1722(17)	O(11)#1−Co(1)−N(31)	92.32(8)	O(42)−Co(2)−O(91)	87.55(7)
Co(1)−N(31)	2.142(2)	O(21)−Co(1)−N(41)#2	90.69(7)	O(22)−Co(2)−O(91)	90.49(7)
Co(1)−N(41)#2	2.150(2)	O(41)−Co(1)−N(41)#2	87.78(7)	O(31)#3−Co(2)−N(21)#4	89.56(7)
Co(2)−O(31)#3	2.0861(17)	O(11)#1−Co(1)−N(41)#2	87.59(7)	O(42)−Co(2)−N(21)#4	94.08(7)
Co(2)−O(42)	2.1005(16)	N(31)−Co(1)−N(41)#2	91.57(8)	O(22)−Co(2)−N(21)#4	85.92(7)
Co(2)−O(22)	2.1208(17)	O(21)−Co(1)−O(91)	92.19(7)	O(31)#3−Co(2)−N(11)	87.27(7)
Co(2)−O(91)	2.1504(18)	O(41)−Co(1)−O(91)	88.08(7)	O(42)−Co(2)−N(11)	86.02(7)
Co(2)−N(11)	2.213(2)	O(11)#1−Co(1)−O(91)	89.47(7)	O(91)−Co(2)−N(11)	93.53(7)
Co(2)−N(21)#4	2.154(2)	N(31)−Co(1)−O(91)	92.50(7)	N(21)#4−Co(2)−N(11)	89.96(8)

[a] Symmetry transformations used to generate equivalent atoms: #1, $-x+1, -y+1, -z$; #2, $-x, -y+1, -z$; #3, $-x+1, -y+1, -z+1$; #4, $-x+1, -y+2, -z+1$.

Scheme 1

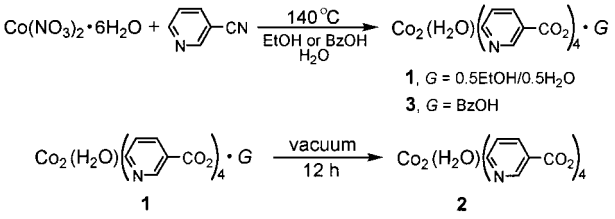

Results and Discussion

Compound **1** was successfully synthesized with a 58% yield based on nicotinate, and the characterization led to the assignment of the formula $Co_2(H_2O)(C_6H_4O_2N)_4 \cdot 0.5CH_3CH_2OH \cdot 0.5H_2O$. Compound **2** was obtained by treating **1** under vacuum and identified using an X-ray crystal diffraction technique. Compound **3** was synthesized in a 62% yield and, on the basis of the characterization, was given the assignment $Co_2(H_2O)(C_6H_4O_2N)_4 \cdot C_6H_5CH_2OH$ (Scheme 1). Under the reaction conditions, 3-cyanopyridine was hydrolyzed to become nicotinate.

Single-crystal X-ray analysis reveals that **1** possesses a three-dimensional porous host framework (Figure 1). The crystallographic asymmetric unit of the Co(II) cluster core consists of two Co(II) centers, four bridging nicotinate ligands, one bridging water molecule, and half of the ethanol and water molecules as guests. The four nicotinate groups adopt two different bridging modes: two nicotinate ligands adopt an exo-tridentate bridging

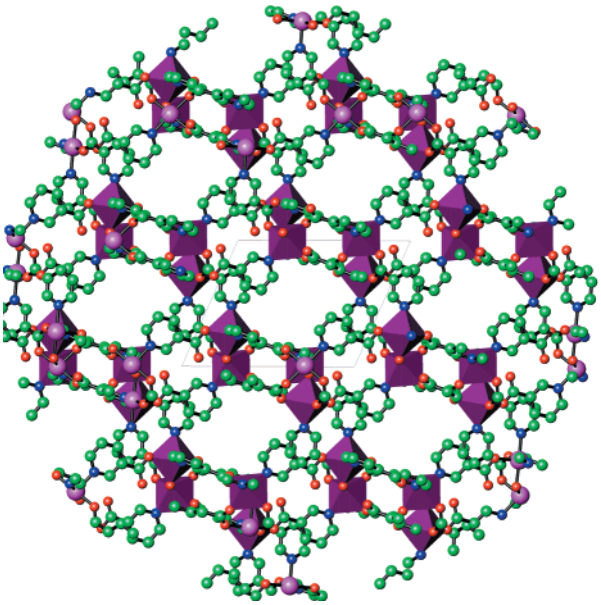

Figure 1. Perspective view of the host structure of **1** along the (100) direction, showing close-packed channels. (Vertex-sharing octahedra: $Co_2O_8N_4$ cluster.)

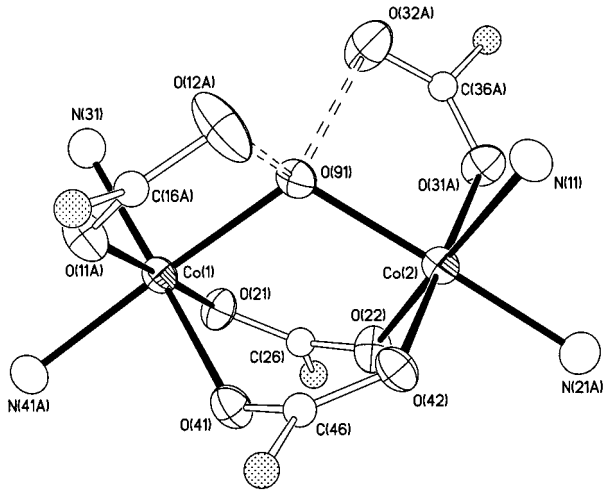

Figure 2. Core unit of the $Co_2O_8N_4$ cluster, showing bridging dicarboxylate groups and a water molecule at 40% ellipsoids. Dashed lines indicated the arrangement of a hydrogen-bonding interaction. Pyridyl groups and hydrogen atoms are omitted for clarity.

mode (with a coordinating pyridyl group and a μ^2,η^2-carboxylato bridge) while the other two adopt an exo-bidentate bridging mode (with a coordinating pyridyl group and a coordinating η^1-carboxylato group). The four nicotinate groups provide a total of 10 binding sites, with the added two sites by a μ^2-bridging water molecule and both of the Co centers adopting a six-coordinated octahedral geometry to become a vertex-sharing (bridging water) $Co_2O_8N_4$ cluster (Figure 2). In addition to the bridging force, the rigidity of the $Co_2O_8N_4$ cluster is further enhanced by hydrogen-bonding interactions between the bridging water molecule and the carboxylate group of nicotinate (O(91)−H···O(12A) and O(91)−H···O(32A) of 2.561 and 2.562 Å, respectively). Two metal centers linked by dicarboxylate bridges can also be seen in nature's example, as in the diiron carboxylate unit in the oxygen-carrying enzyme hemerythrin.[37]

Within the one-dimensional channels of **1**, ethanol and water molecules occupy the channels with an estimated cross-sectional area of about 10.8 × 4.5 Å (Figure 3).[38] Attempts were made to remove the guests to form Co(II)$_2$(nicotinate)$_4$ (**2**) by treating the same single crystal of **1** under vacuum for 12 h. The structure of **2** remains intact, even after the removal of the guest as revealed by single-crystal X-ray analysis. Linkage of the $Co_2O_8N_4$ clusters with nicotinate ligands assembles the channel space. Particularly, nicotinate ligands are arranged in a "double-wall" fashion favoring a $\pi-\pi$ interaction. This nicotinate double wall can further enhance the robustness of the host so that it can survive the highly porous status in the absence of guests. (The host framework atoms of **2** only occupy about 58% of the unit cell volume based on PLATON analysis.)[39] The effective cavity space can also accommodate larger guest molecules of different sizes and shapes such as benzyl alcohol (BzOH) as in Co(II)$_2$(nicotinate)$_4$·BzOH (**3**).

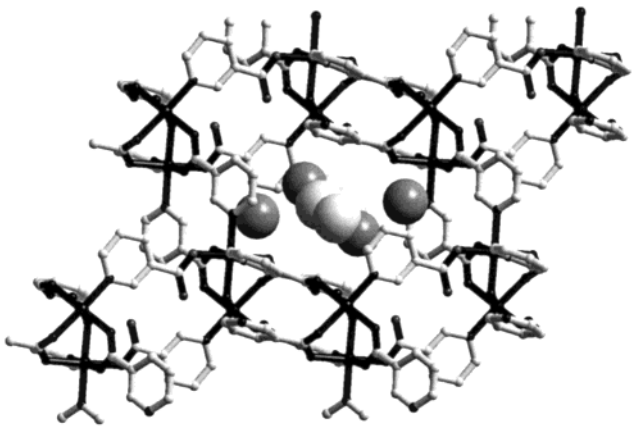

Figure 3. Graphical representation of the host assembly based on the crystallographic results of **1** (black, $Co_2O_8N_4$ clusters; gray, nicotinate ligand). About 10.8 × 4.5 Å of the channel cross section is capable of guest inclusion (ethanol and water molecules). For clarity, hydrogen atoms are omitted.

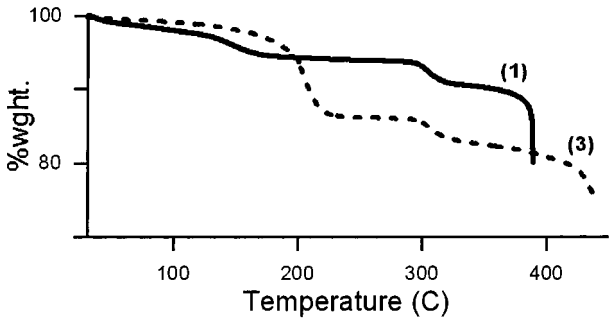

Figure 4. Thermogravimetric diagram of compounds **1** and **3**.

TG analysis agrees well with the crystallographic observations (Figure 4). The TG curve of **1** illustrates the release of the guest (ethanol and water) molecules (calcd 4.9%, found 5.3%) between 50 and 200 °C, followed by the release of bridging water (calcd 2.8%, found 3.0%) upon heating to 295 °C. For **3**, the release of benzyl alcohol occurred between 90 and 210 °C (calcd 14.2%, found 13.6%), and the loss of bridging water occurred at 295 °C.

The existence of a plateau area (about 90 °C duration) between the two losses observed in the TG analysis for compounds **1** and **3** allows the selective study of the desorption−sorption process. A freshly ground sample of **1** was heated at 250 °C for 4 h and then was naturally cooled to room temperature by exposing the sample in the atmosphere for 20 h. The framework integrity is sustained as observed by the PXRD results (Figure 5).

Choosing a spacer ligand with an appropriate shape and length as the linker of metal centers is also an important factor for the construction of robust frameworks possessing open cavities. Similar to **1**, the structure of cadmium(II) (4-(3-pyridyl)-ethenylbenzoate) (**4**) possesses the same type of binuclear metal-cluster core.[40] However, the framework of **4** presents a different spatial arrangement than that induced by the organic linker as compared to **1**. No cavities have been observed in the cadmium case.

The inverse magnetic susceptibilities and effective moments per mole of cobalt for complexes **1** and **3** are given in Figure 6. The effective moments per mole of cobalt are around 5.0 μ_B at 300 K and decrease with decreasing temperature, which is a

(34) *International Tables for X-ray Crystallography*; Kluwer Academic Publishers: Dordrecht, The Netherlands, 1989; Vol. C.
(35) Farrugia, L. J. *J. Appl. Crystallogr.* **1999**, *32*, 837.
(36) Sheldrick, G. M. *SHELX-97: Including SHELXS and SHELXL*; University of Göttingen: Göttingen, Germany, 1997.
(37) Lippard, S. J.; Berg, J. M. *Principles of Bioinorganic Chemistry*; University Science Books: Mill Valley, CA, 1994.
(38) This is a simplified view, which is derived based on the geometrical calculation of the distance of the nuclei available from crystallographic data. van der Waals radii of 1.5, 1.7, and 1.8 Å for O, N, and C atoms, respectively, are exploited.
(39) Spek, A. L. *PLATON: A Multipurpose Crystallographic Tool*; Utrecht University: Utrecht, The Netherlands, 1998.
(40) Evans, O. R.; Lin, W. *J. Chem. Soc., Dalton Trans.* **2000**, 3949.

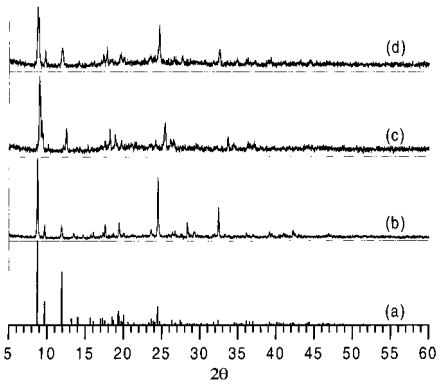

Figure 5. (a) Simulated PXRD pattern. (b) PXRD of a freshly grounded sample of **1**. (c) After the heating of **1** at 250 °C for 4 h. (d) After the exposure of the heated sample to the atmosphere at room temperature for 20 h.

typical behavior of the antiferromagnetically coupled magnetic pair. At the first approximation, we apply the results of Curie−Weiss's law from the high-temperature magnetic susceptibilities data to measure the magnetic coupling interaction

$$\chi = \frac{Ng^2\beta^2 S(S+1)}{3k_B T - 2JS(S+1)} = \frac{C_M}{T-\theta} \qquad (1)$$

where N, g, β, and k_B have their usual meanings and J is the exchange interaction between the metal ions.[41] The 20.0−300 K temperature dependencies of the magnetic susceptibilities of **1** and **3** were fit by the Curie−Weiss expression with C_M values of 3.17 and 3.42 emu K/mol and θ values of −31.3 and −33.1 K, respectively. The negative θ values indicate the antiferromagnetic coupling between the metal sites. According to the equations, the effective moment $\mu_{eff} = (8C_M)^{1/2}$ and the exchange coupling constant $J/k_B = 3\theta/[2S(S+1)]$ would be obtained. These calculated values of μ_{eff} and J/k_B are 5.0 and 5.2 μ_B and −12.5 and −13.2 K for complexes **1** and **3**, respectively. The values of μ_{eff} are larger than the spin-only value of 3.78 μ_B, and this is commonly observed for the Co^{2+} centers, which is due to incomplete quenching and arises from the spin−orbital coupling.[42] The magnetic coupling constant J/k_B is around −13 K and indicates that there is antiferromagnetic coupling via the bridging dicarboxylate groups and the water within the cobalt metal centers. The antiferromagnetic exchange interactions may be through Co(1)−O(91)−Co(2) with an angle of 113.6°, in which a large superexchange angle leads to an antiferromagnetic interaction.

To analyze the magnetic exchange coupling interaction between the cobalt dimer, the susceptibility data of the complexes are fitted with the binuclear magnetic equations[43]

$$\chi = \frac{Ng^2\beta^2}{k_B T}\frac{14 + 5X^6 + X^{10}}{7 + 5X^6 + 3X^{10} + X^{12}} + \mathrm{TIP} \qquad (2)$$

where $X = \exp(-J/k_B T)$ and TIP is the temperature-independent paramagnetism of the Co^{2+} ion. The reasonable fitting results for magnetic susceptibility data above 50.0 K with TIP = 200 × 10^{-4} emu/mol are $g = 2.53$ and $J = -7.9$ K for complex **1** and $g = 2.63$ and $J = -8.3$ K for complex **3**. The negative values of J indicate the antiferromagnetic nature, and the spin−orbital coupling contributes to the trivial g factor. However, the exchange coupling parameters J obtained from two approximations are different. This divergence would be associated with the complicated cobalt system, which has the following properties: (i) ligand-field splitting of the free ion, (ii) spin−orbital coupling, and (iii) an anisotropic intra- and interdimer exchange interaction.[41]

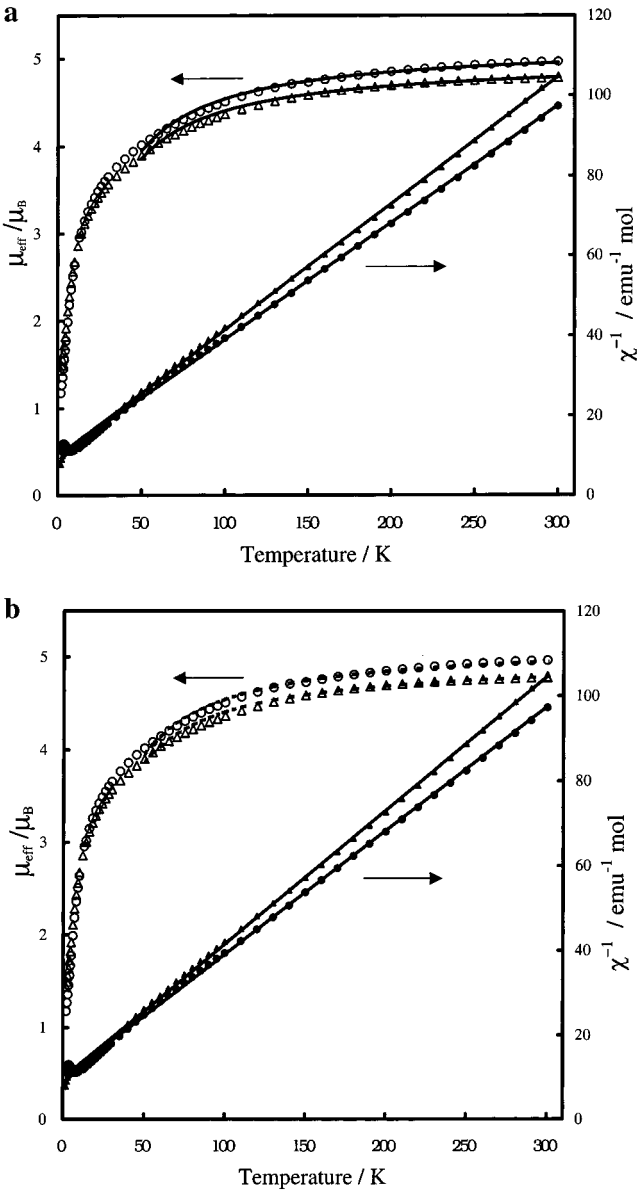

Figure 6. Magnetic effective moment versus temperature plots for complexes **1** (△) and **3** (○) and inverse magnetic susceptibility versus temperature plots for complexes **1** (▲) and **3** (●) at a field of 1000 G. (a) The solid lines represent the best fitting to the Curie−Weiss law for the inverse-susceptibility data of 20−300 K. (b) The dashed lines represent the best fitting to eq 2 for susceptibility data of 50.0−300 K.

Conclusions

In summary, a new robust porous host framework, $Co_2(H_2O)(C_6H_4NO_2)_4$, has been successfully synthesized and characterized. It contains nanoscale cavities that can accommodate guest molecules of various shapes and sizes. Taking advantage of the rigid cluster unit and an appropriate organic spacer, the building of a robust host that can withhold high porosity becomes feasible. Exploration of the binding nature of diverse metal centers with organic ligands to assemble a novel

(41) Kahn, O. *Molecular Magnetism*; VCH: New York, 1993.
(42) Carlin, R. L *Magnetochemistry*; Springer-Verlag: New York, 1986.
(43) Yang, L.; Jin, W.; Lin, J. *Polyhedron* **2000**, *19*, 93.

cluster-type building-block unit to form networks with a tailored functionality is currently undertaken.

Acknowledgment. We thank Academia Sinica, Chinese Petroleum Corp., and the National Science Council, the Republic of China, for financial support.

Supporting Information Available: Figures of the asymmetric unit of **1** and a packing plot of **3** and X-ray crystallographic files in CIF format for the structures of **1**−**3**. This material is available free of charge via the Internet at http: //pubs.acs.org.

IC010528K